

SHORT THESIS FOR THE DEGREE OF DOCTOR OF PHILOSOPHY (PHD)

**Effects of Bacterial Secondary Metabolites on Clinically
Relevant *Candida* Species**

by Fruzsina Kovács

Supervisor: Renátó Kovács, PhD



UNIVERSITY OF DEBRECEN

DOCTORAL SCHOOL OF PHARMACEUTICAL SCIENCES

DEBRECEN, 2026

Effects of Bacterial Secondary Metabolites on Clinically Relevant *Candida* Species

by Kovács Fruzsina molecular biology MSc

Supervisor: Renátó Kovács, PhD

Doctoral School of Pharmaceutical Sciences, University of Debrecen

Head of the **Defense Committee:** Béla Juhász, PhD, DSc

Reviewers: Marianna Domán, PhD

Melinda Paholcsek, PhD

Members of the Defense Committee: Enikő Fehér, PhD

István Varga, PhD

The PhD Defense takes place at the Lecture Hall of the Department of Internal Medicine Building “A”, Faculty of Medicine, University of Debrecen, on 1st of April 2026, at 13:00

Introduction

Interactions between bacteria and fungi encompass a variety of relationships, such as symbiosis, antagonism, and competition, all of which occur in both natural and artificial environments. In living organisms, bacterial–fungal interactions are typically discussed in the context of symbiotic associations that maintain the composition and stability of the normal microbiota. However, bacteria and fungi do not always coexist harmoniously. When environmental conditions change—such as during infection, antibiotic treatment, or exposure to other stress factors—biological defence mechanisms are activated, often leading to antagonistic interactions. Studying these antagonistic relationships not only deepens our understanding of the ecological principles governing microbial communities but also provides valuable insights for developing new strategies in the prevention and treatment of infectious diseases.

Bacteria–fungi-associated infections represent a serious burden on human health and the healthcare system, which explains the growing interest in the detailed investigation of these interactions. Numerous clinical studies have reported the increasing occurrence of polymicrobial infections involving *Candida* species. According to published data, more than 20% of patients suffering from invasive candidiasis have a polymicrobial infection in the background. It is well known that *Candida* species often colonize various anatomical sites of the human body together with bacterial species.

Polymicrobial interactions have become a key focus of microbiological research in recent years. As resistance to both antibacterial and antifungal agents continue to increase worldwide, there is a pressing need for a more detailed understanding of microbial interactions — particularly those that influence the pathogenesis and therapeutic targeting of *Candida*-associated polymicrobial infections.

There is substantial evidence supporting the central role of commensal *Candida albicans* residing in the intestinal tract in the development of systemic candidiasis. One of the main virulence factors of *C. albicans* is its morphological plasticity — the ability to switch from yeast to filamentous form. Following adhesion to host cells, yeast cells form hyphae that can penetrate the intestinal mucosa, allowing the fungus to invade deeper tissue layers and cause invasive infection. Several studies have demonstrated that bacterial metabolites produced by members of the normal gastrointestinal microbiota can inhibit *C. albicans* virulence, thereby contributing to the maintenance of microbial and intestinal homeostasis.

As a result of these antifungal properties, increasing attention has been directed toward potentially probiotic species, such as *Bacillus subtilis*. On the one hand, *B. subtilis* spores are known to modulate host immune responses; on the other hand, its vegetative cells release enzymes, antioxidants, and vitamins that support digestion. In addition to the immunomodulatory effects of *B. subtilis* exopolysaccharides, they may also prevent inflammatory diseases triggered by enteric pathogens. Moreover, several *B. subtilis* strains are capable of secreting antimicrobial compounds that help maintain optimal microbial balance. Overall, *B. subtilis* is considered an effective natural source of antifungal compounds, including those active against *Candida* species.

Among these natural compounds, surfactin is a cyclic lipopeptide produced by *B. subtilis* that primarily exhibits activity against Gram-positive bacteria. Recent studies have revealed that surfactin also affects yeast cells, as it effectively reduces the adhesion and surface hydrophobicity of *C. albicans*. However, the impact of surfactin on *C. albicans* has not been comprehensively investigated, and the molecular mechanisms underlying its physiological effects remain poorly understood. Understanding how surfactin influences the physiological and genetic characteristics of *C. albicans* could be crucial for the future development of probiotic formulations.

One of the best-studied models of antagonistic bacteria–fungus interactions is that between *Pseudomonas aeruginosa* and *C. albicans*. Both microbes can be part of the normal flora and often co-colonize various anatomical sites of the host. Since both species are capable of forming biofilms, they are frequently associated with invasive infections related to indwelling medical devices. Previous studies have identified *N*-(3-oxododecanoyl)-*L*-homoserine lactone (HSL), a quorum-sensing molecule produced by *P. aeruginosa*, as a key factor responsible for antifungal activity. HSL serves as the primary quorum-sensing signal molecule of *P. aeruginosa* and plays a pivotal role in regulating bacterial virulence factor production. Within the *Pseudomonas*–*Candida* interaction, HSL has been shown to inhibit *C. albicans* hyphal formation, reduce biofilm development, and induce apoptosis in fungal cells. However, these HSL-mediated effects described for *C. albicans* may not necessarily be extrapolated to other non-*albicans* species, as shown previously for other molecules and compounds.

Among the non-*albicans* species, *Candida auris* is one of the most concerning and rapidly emerging pathogens. Since its identification in 2009, it has been reported in nearly all regions of the world and has become a serious global public health threat due to its rapid spread. Unlike other *Candida* species, *C. auris* displays remarkable adaptability to extreme environmental

conditions and efficiently colonizes both biotic and abiotic surfaces. Its high resistance to most antifungal agents contributes to the emergence of difficult-to-control nosocomial outbreaks associated with *C. auris* infections.

Previous studies have shown that skin surfaces colonized by *C. auris* exhibit a significant reduction in the abundance of commensal Gram-positive species, while Gram-negative bacteria — particularly *P. aeruginosa* — become dominant. Despite these observations, there is currently insufficient information on whether *P. aeruginosa* affects the physiological properties of *C. auris*, or whether its quorum-sensing molecule, HSL, can directly interact with *C. auris* cells.

Based on the data summarized above, this dissertation presents a comprehensive physiological and molecular analysis aimed at investigating the antifungal activity of secondary metabolites and/or quorum-sensing molecules produced by various bacterial species against two clinically significant *Candida* species. In the first phase of our research, we examined the antifungal properties of surfactin, a secondary metabolite derived from *B. subtilis*, against *C. albicans*. In the second phase, we focused on the effects of HSL, a quorum-sensing molecule from *P. aeruginosa*, on *C. auris*. We hope that our findings will contribute to the development of innovative therapeutic approaches against *Candida* infections and provide insights into the physiological and molecular differences among species within the *Candida* genus.

Objectives

According to data from the scientific literature, it can be concluded that quorum-sensing molecules and other secondary metabolites secreted by certain bacterial species can possess antifungal properties, inhibiting both the growth and viability of neighboring fungal cells.

Considering these aspects, the primary aim of our experimental work was to explore the extent to which quorum-sensing molecules and bacterial secondary metabolites are capable of inhibiting the development of infections caused by *C. albicans* and *C. auris*, and to identify the possible mechanisms underlying their antifungal activity.

In the first part of our research, we investigated the effects of surfactin, a secondary metabolite produced by the potentially probiotic bacterium *Bacillus subtilis*, on the growth, morphology, and virulence of *C. albicans*.

In the second part of the study, we analysed the inhibitory effects of N-(3-oxododecanoyl)-L-homoserine lactone (HSL) — a quorum-sensing molecule produced by *Pseudomonas aeruginosa* — on *C. auris*, and compared these findings with the results obtained for *C. albicans*.

Materials and Methods

Isolates and Culture Conditions

For the experiments, the *Candida auris* isolate belonging to the South Asian (Indian) clade (NCPF 8973) and the reference strain *Candida albicans* (SC5314) were used. The *C. auris* isolates included in our strain collection were obtained from the United Kingdom National Mycology Reference Laboratory, and clade-level classification of the isolates was performed by Andrew M. Borman and colleagues based on sequencing data of the 28S rRNA and/or ITS1 regions (Borman et al., 2017). Both fungal strains were cultured on Sabouraud dextrose agar at 37 °C (medium composition: 1% peptone, 4% dextrose, 1.5% agar, 0.4% chloramphenicol, pH 5.6 ± 0.2 ; Thermo Fisher Scientific, Waltham, USA).

Growth of *Candida* cells under different treatments

During the experiments, surfactin (Merck, Budapest, Hungary) was applied at a final concentration of 128 mg/L, corresponding to the physiological range produced by different *Bacillus subtilis* strains. HSL (Merck, Budapest, Hungary) was tested in a concentration range of 50–200 μM — both sub-physiological (50–100 μM) and physiological (200 μM) levels — under *in vitro* and *in vivo* conditions. The tested concentrations were prepared in solvents recommended by the manufacturer: surfactin was dissolved in ethanol, and HSL in dimethyl sulfoxide (DMSO; VWR, Debrecen, Hungary). The final solvent concentration did not exceed 1% (v/v) in any treatment, ensuring that observed inhibitory effects were solely attributable to the biological activity of surfactin and HSL.

Pre-cultured *C. albicans* and *C. auris* cells were grown overnight in 5 mL YPD liquid medium (Yeast Peptone Dextrose; Merck, Budapest, Hungary) at 37 °C. Cultures were then diluted to an optical density of 0.1 (OD_{640}) and incubated in 100 mL Erlenmeyer flasks containing 20 mL medium at 37 °C with shaking at 2.3 Hz. After 4 hours of incubation, surfactin was added to reach a final concentration of 128 mg/L. In HSL-based experiments, 100 μM and 200 μM final concentrations were tested. Microbial growth was monitored by measuring the optical density (OD_{640}) at defined time points. Cultures were harvested after 4 hours of treatment for intracellular metal quantification and transcriptomic analyses.

Effect of Surfactin on *Candida albicans* morphology

In parallel with the growth assays, the effect of surfactin on *C. albicans* morphology was investigated. Cells were cultured in RPMI-1640 liquid medium (Roswell Park Memorial Institute 1640 medium; Thermo Fisher Scientific, Waltham, USA) on 8-well Permanox chamber slides at 37 °C (Lab-Tek® Chamber Slide™ System; VWR, Debrecen, Hungary). Surfactin treatment was applied at time 0 h at a final concentration of 128 mg/L, and samples were collected at 4, 5, 6, and 8 hours. After incubation, chambers were washed with sterile physiological saline, a drop of immersion oil (10 µL) was added, and morphological changes were examined under a phase-contrast microscope (Zeiss Axioskop 2 MOT with Zeiss AxioCam HRc camera). Images were captured using Zeiss Axiovision 4.8.2 software.

Adhesion and early biofilm formation of *Candida* cells following HSL Treatment

To quantify the metabolic activity of sessile *Candida* cells, isolates were cultured in RPMI-1640 medium (Thermo Fisher Scientific, Waltham, USA) in sterile 96-well microplates (TPP, Trasadingen, Switzerland). *C. albicans* and *C. auris* suspensions were adjusted to 1×10^6 cells/mL, and 100 µL aliquots were added per well. Plates were incubated at 37 °C for 2, 4, 6, and 8 hours. HSL treatment was applied at time 0 h at final concentrations of 100 µM and 200 µM. After incubation, cultures were washed with sterile physiological saline, and the metabolic activity of adherent cells was determined using the [2,3-bis(2-methoxy-4-nitro-5-sulphophenyl)-2H-tetrazolium-5-carboxanilide] assay (XTT assay) (Georgiou et al., 1992; Hawser, 1996). Measurements were performed at 492 nm using a Multiskan Sky microplate spectrophotometer (Thermo Fisher Scientific, Waltham, USA). Metabolic activity was calculated as a percentage based on absorbance values:

$$100\% \times (A_{\text{sample}} - A_{\text{background}}) / (A_{\text{untreated}} - A_{\text{background}}),$$

where *A* denotes the absorbance reading. Experiments were conducted in triplicate, and mean ± SD values were calculated for all time points.

Metabolic assays were complemented by wide-field fluorescence microscopy. Adhesion of *C. albicans* and *C. auris* cells was examined on 8-well Permanox chamber slides under static conditions at 37 °C after 24 hours of incubation (Lab-Tek® Chamber Slide™ System; VWR, Debrecen, Hungary). HSL was added at time 0 h (100 µM and 200 µM final concentrations), and samples were analysed at 2, 4, 6, and 8 hours. After incubation, chambers were washed with sterile saline, and cells were stained with Calcofluor White (3 mg/mL; Thermo Fisher Scientific, Waltham, MA, USA), a fluorescent dye binding specifically to chitin in the fungal

cell wall. After 30 minutes of incubation at 37 °C, a drop of immersion oil (10 µL) was added, and morphological changes were documented using a Zeiss Axioskop 2 MOT fluorescence microscope with a Zeiss AxioCam HRc camera. Images were processed using Zeiss Axiovision 4.8.2 software.

Determination of intracellular metal content after Surfactin or HSL treatment

Fungal cell cultures and treatments with surfactin or HSL were performed as described previously. After 4 hours of exposure, cells were collected by centrifugation (5 min, 4000 g, 4 °C), lyophilized, and analysed for intracellular metal content—iron (Fe), zinc (Zn), copper (Cu), and manganese (Mn)—using inductively coupled plasma optical emission spectrometry (ICP-OES; 5110 Agilent Technologies, Santa Clara, CA, USA) following the protocols of Jakab et al. (2021, 2024). Lyophilized biomass was weighed on an analytical balance (Precisa ES 225SM-DR) and subjected to atmospheric wet digestion using 3 mL of 65% nitric acid (HNO₃; Merck, Budapest, Hungary) and 1 mL of 30% hydrogen peroxide (H₂O₂; Merck, Budapest, Hungary). Digested samples were transferred quantitatively into plastic centrifuge tubes and diluted to 12 mL with 0.1 M HNO₃ prepared in ultrapure water (Synergy UV; Merck, Budapest, Hungary). Samples were stored at room temperature until ICP-OES analysis. Intracellular metal contents were expressed in DCM units (mg/kg dry cell mass) based on triplicate measurements (mean ± SD). (The section continues in the same structured manner for the *in vivo* studies, RNA isolation, RNA-seq, GSE analysis, RT-qPCR, and statistical analysis.)

Effect of HSL on *Candida virulence in vivo*

For *in vivo* studies, immunosuppressed female BALB/c mice (21–23 g; Charles River Laboratories, Wilmington, MA, USA) were used to assess the effect of HSL exposure on *C. auris* virulence and to compare with *C. albicans*. Animals were maintained in accordance with the Guide for the Care and Use of Laboratory Animals, and experiments were approved by the Workplace Animal Welfare Committee of the University of Debrecen (permits: 12/2014 DEMÁB and 8/2024 DEMÁB). Permanent immunosuppression was induced by intraperitoneal cyclophosphamide: 150 mg/kg on day –4 relative to infection, 100 mg/kg on day –1, and 100 mg/kg on days +2 and +5. Infections were performed intravenously via the lateral tail vein at doses of 8×10^6 CFU/mouse for *C. auris* and 2×10^4 CFU/mouse for *C. albicans*. HSL treatments (50, 100, or 200 µM in 0.5 mL physiological saline) began 24 h post-inoculation and were administered intraperitoneally once daily for 5 consecutive days, corresponding to

approximately 0.35, 0.70, and 1.40 mg/kg. Control animals received sterile physiological saline. On day 6 post-infection, mice were euthanized by cervical dislocation. Kidneys were excised, weighed, and homogenized aseptically. Ten-fold serial dilutions were plated (100 μ L) onto Sabouraud dextrose agar (VWR, Debrecen, Hungary) and incubated for 48 h at 37 °C (Jakab et al., 2019; Nagy et al., 2020). Colony counts were used to determine viable fungal burden; the detection limit was 100 CFU/g tissue. Both treated and untreated kidneys were submitted for histopathology to the Department of Pathology, Kenézy Gyula Campus, Clinical Center, University of Debrecen. From formalin-fixed, paraffin-embedded tissue blocks, 4 μ m sections were prepared and stained with hematoxylin–eosin and periodic acid–Schiff (PAS) to visualize fungal elements.

RNA isolation

As in the growth assays, after 4 h surfactin or HSL treatment, *Candida* cells from 20 mL cultures were collected by centrifugation (5 min, 4000 g, 4 °C), washed three times with ice-cold sterile physiological saline, and stored at –70 °C until processing. Total RNA was isolated from lyophilized cells (CHRIST Alpha 1–2 LDplus lyophilizer; Osterode, Germany) using the method of Chomczynski (1993) and following the manufacturer’s protocol for the Eukaryotic Total RNA Nano Kit. RNA quality and quantity were assessed at the Genomic Medicine and Bioinformatics Service Laboratory, Faculty of Medicine, University of Debrecen, using a NanoDrop ND-1000 spectrophotometer (Thermo Scientific, USA) and an Agilent 2100 BioAnalyzer (Agilent Technologies, Santa Clara, CA, USA).

Next-Generation RNA Sequencing (RNA-seq)

Library preparation, sequencing, and data analysis were performed at the Institute of Biochemistry and Molecular Biology, Faculty of Medicine, University of Debrecen, within the Genomic Medicine and Bioinformatics Center. Libraries were prepared from 0.25 μ g high-quality total RNA using the NEBNext RNA Sample Preparation Kit (New England Biolabs, Ipswich, MA, USA). Sequencing was performed on an Illumina NextSeq 500 (Illumina, San Diego, CA, USA) generating 75-bp reads. We obtained 22.5–31.4 million reads for *C. albicans* and 18.6–23.1 million reads for *C. auris* samples. Raw data quality was assessed with FastQC (Andrews, 2010). Reads were aligned using HISAT2 v2.1 and SAMtools to the *C. albicans* SC5314 (GCF_000182965.3) and *C. auris* B8441 (GCA_002759435.2) reference genomes (NCBI). Alignment rates were \geq 93% for all samples. Data processing and normalization were performed in StrandNGS 4.0. Normalized transcript levels were calculated using DESeq2.

Differentially expressed genes (DEGs) were identified by *t*-tests with Benjamini–Hochberg FDR correction; genes with $p < 0.05$ and fold change (FC) > 1.5 or < -1.5 were considered significant. Principal component analysis (PCA) of transcriptomes was also performed in StrandNGS 4.0. RNA-seq datasets are available in the Gene Expression Omnibus (GEO). Results for surfactin treatment are under series GSE199383, and those for HSL treatment under GSE271513.

Gene Set Enrichment (GSE) analysis

Biological processes associated with up- and downregulated genes were examined by functional gene set enrichment using the Candida Genome Database Gene Ontology Term Finder (<http://www.candidagenome.org>) and FungiDB (<https://fungidb.org>). GO, FunCat (Functional Catalogue), and KEGG categories were analyzed with FungiFun2 v2.2.8. Only results with adjusted *p*-values < 0.05 were considered.

Quantitative Reverse Transcription PCR (RT-qPCR)

RT-qPCR was used to validate transcriptional changes induced by surfactin and HSL. Reactions were performed with the Luna Universal One-Step RT-qPCR Kit (New England Biolabs, Ipswich, MA, USA) following the manufacturer's instructions. Each reaction contained 500 ng DNase-treated (Sigma-Aldrich, St. Louis, MO, USA) total RNA and 0.4 μM gene-specific primer pairs (Appendices 1 and 2). Reaction mixture: 10 μL reaction mix, 1 μL enzyme mix, 0.8 μL each of 10 μM forward and reverse primers, 5 μL template RNA, and nuclease-free water to 20 μL . All samples were analyzed in three independent biological replicates. Primers were designed using Oligo Explorer (v1.1) and Oligo Analyzer (v1.0.2). Reactions were run on a LightCycler 480 II real-time PCR system (Roche, Basel, Switzerland). Relative transcript levels were calculated by the $\Delta\Delta\text{Ct}$ method: $\Delta\Delta\text{Ct} = \Delta\text{Ct}_{\text{treated}} - \Delta\text{Ct}_{\text{untreated}}$, where $\Delta\text{Ct} = \text{Ct}_{\text{target}} - \text{Ct}_{\text{reference}}$. An increase in $\Delta\Delta\text{Ct}$ indicates elevated relative transcription in the treated sample versus the untreated control. Endogenous controls were C2_02740C (HPT1) and C1_13700W (ACT1) for *C. albicans*, and B9J08_000486 (ACT1) for *C. auris*.

Statistical analysis

Growth experiments and intracellular metal measurements were performed in triplicate and are reported as mean \pm SD. Differences between treated and untreated samples were evaluated by paired Student's *t*-tests (GraphPad Prism 10.0). $P < 0.05$ was considered statistically significant. For *in vivo* experiments, kidney fungal burdens were analyzed by Kruskal–Wallis test with

Dunn's post hoc test ($p < 0.05$). For gene enrichment analyses, Fisher's exact test was applied using R (v4.1.1) and the stats package (v3.5.3). Genes with fold change ≥ 1.5 and $p < 0.05$ were considered relevant. Graphs were generated in GraphPad Prism 10.0.

Results

Effect of Surfactin on the growth and morphology of *Candida albicans*

In the first phase of our experimental work, we investigated the effect of surfactin at a final concentration of 128 mg/L on the growth of *Candida albicans* at different exposure times. Following a 4-hour pre-cultivation period, the fungal cultures were treated with surfactin, and growth was monitored after 1, 2, and 4 hours of exposure by measuring both optical density and dry cell mass (DCM). The results demonstrated that surfactin inhibited fungal growth even after 1 hour of incubation, as evidenced by reduced optical density (control: 0.96 ± 0.04 ; treated: 0.75 ± 0.02 at OD₆₄₀) and decreased DCM values (control: 0.95 ± 0.10 g/L; treated: 0.60 ± 0.15 g/L; $p < 0.01$). This significant inhibitory effect remained observable at later time points as well — after 6 hours (control: 1.5 ± 0.2 g/L; treated: 0.7 ± 0.1 g/L) and 8 hours (control: 3.2 ± 0.3 g/L; treated: 1.0 ± 0.2 g/L; $p < 0.01$ – 0.001).

Microscopic observations revealed marked morphological alterations between treated and untreated cultures. Hyphal and pseudohyphal forms—key morphological features of *C. albicans* virulence—were significantly less frequent in the surfactin-treated samples. Quantitative analysis showed that after 8 hours of incubation, the proportion of true hyphae decreased from $14.33\% \pm 1.53\%$ (control) to $10.33\% \pm 2.08\%$ ($p < 0.05$), while pseudohyphal forms dropped from $29.66\% \pm 3.06\%$ to $22.67\% \pm 3.05\%$ ($p < 0.05$). These findings indicate that surfactin effectively interferes with the dimorphic transition of *C. albicans*.

Transcriptional Changes in *Candida albicans* Following Surfactin Treatment

RNA sequencing analysis revealed that surfactin significantly altered gene transcription patterns in *C. albicans*, inducing large-scale transcriptomic changes. Comparative analysis between treated and untreated cultures identified 1,389 differentially expressed genes (DEGs) — of which 773 were upregulated and 617 were downregulated.

Functional categorization of these genes showed that surfactin predominantly affected genes involved in transmembrane transport. Among the upregulated genes, we identified multiple multidrug transporters (e.g., *MDR1* and *FLU1*) and genes related to carbohydrate transport (*HGT1*, *HGT10*, *HGT14*, *HGT18*, *HXT5*, *NAG3*, *SFC1*, *GAL102*).

In addition, genes associated with oxidative stress responses, such as those involved in glutathione metabolism (*GTT11*, *GTT12*, *GTT13*, *GCS1*, *GST2*, *C5_01560C*, *TTR1*), showed increased transcription. Genes regulating intracellular metal homeostasis—particularly those related to iron, copper, and zinc — were also upregulated. These included iron reductases

(*CFL4*, *CFL11*, *CR_07300W*, *C7_00430W*, *FRE7*, *FRE9*), copper oxidases (*FET99*, *CCC2*), siderophore transporters (*SIT1*), and the transcription factor *SEF1*. Similarly, *MAC1* (a copper-regulating transcription factor), copper chaperones (*CCS1*, *CTR1*, *CCC2*), and zinc-related genes (*CSRI*, *PRA1*) exhibited elevated expression levels following surfactin treatment.

Conversely, several genes linked to metal uptake and storage showed decreased transcription, including ferri-permeases (*FTR1*, *FTR2*), hem utilization genes (*HMX1*, *PGA10*, *CSA1*), the transcription factor *AFT2*, and vacuolar transporters for iron (*SMF3*), copper (*CRP1*), and zinc (*ZRT1*).

Surfactin treatment also affected genes associated with adhesion and biofilm formation. Nine genes related to biofilm structure and regulation were downregulated, including *EAP1* and *PGA1* (adhesion), *EFG1*, *ROB1*, *CPH2*, *IFD6*, *GCA1*, and *ADH5* (biofilm maturation), and *NRG1* (biofilm dispersion).

Furthermore, genes associated with ribosomal protein synthesis and RNA export (*RPS3*, *RPS5*, *RPS10*, *RPS15*, *RPS18*, *RPS19A*, *RPS21*, *RPS26A*, *RPS28B*, *YST1*) were markedly downregulated, which likely contributed to the observed reduction in metabolic activity. Validation of the RNA-seq results by RT-qPCR showed strong correlation (Pearson's $r = 0.95$) across the 15 analysed genes.

Effect of Surfactin on the intracellular metal concentration of *Candida albicans*

Because transcriptomic data indicated significant changes in genes regulating metal ion homeostasis, we quantified intracellular metal concentrations after 4-hour surfactin exposure using ICP-OES. Results confirmed that intracellular iron, manganese, and zinc levels were significantly reduced compared with untreated controls ($p < 0.05$ – 0.01). Iron concentration decreased from $127.1 \pm 18.4 \mu\text{g/g}$ (control) to $70.9 \pm 8.4 \mu\text{g/g}$ (treated; $p < 0.05$). Zinc concentration dropped from $214.4 \pm 4.5 \mu\text{g/g}$ to $169.6 \pm 8.9 \mu\text{g/g}$ ($p < 0.01$), while manganese content decreased from $8.1 \pm 0.5 \mu\text{g/g}$ to $5.3 \pm 1.3 \mu\text{g/g}$ ($p < 0.05$). In contrast, no statistically significant difference was observed in copper content (control: $3.1 \pm 0.95 \mu\text{g/g}$; treated: $2.0 \pm 0.25 \mu\text{g/g}$; $p > 0.05$). These data support that surfactin disrupts metal ion homeostasis in *C. albicans*, likely contributing to its antifungal activity.

Effect of HSL on the growth of *Candida albicans* and *Candida auris*

The growth of planktonic *C. auris* and *C. albicans* cells was assessed following treatment with HSL at concentrations of $100 \mu\text{M}$ and $200 \mu\text{M}$. When HSL was added to pre-cultured *Candida* cells, a pronounced inhibitory effect was observed after only 2 hours of exposure. This growth

inhibition was confirmed by decreases in both optical density (OD₆₄₀) and dry cell mass (DCM). For *C. auris*, OD₆₄₀ values in untreated controls were 1.06 ± 0.03 , compared with 0.97 ± 0.02 and 0.82 ± 0.01 for 100 μM and 200 μM HSL treatments, respectively ($p < 0.001$ – 0.01). DCM values also decreased significantly: from 0.26 ± 0.02 g/L in untreated samples to 0.13 ± 0.02 g/L and 0.09 ± 0.02 g/L following 100 μM and 200 μM HSL treatments ($p < 0.001$). In contrast, *C. albicans* showed significant growth inhibition only at 200 μM HSL after 2 hours of exposure. OD₆₄₀ absorbance decreased from 1.33 ± 0.04 (control) to 1.24 ± 0.03 ($p < 0.01$), and DCM decreased from 0.54 ± 0.03 g/L to 0.46 ± 0.02 g/L ($p < 0.01$). These results indicate that *C. auris* is more sensitive to HSL exposure than *C. albicans* under the tested conditions.

Effect of HSL on biofilm formation by *Candida albicans* and *Candida auris*

HSL treatment inhibited the metabolic activity of sessile *Candida* cells in a concentration-dependent manner. In *C. auris*, all tested concentrations reduced metabolic activity relative to the control, whereas in *C. albicans*, inhibition increased proportionally with concentration. After 8 hours of HSL exposure, the metabolic activity of adherent *C. auris* cells decreased to $64.8\% \pm 2.5\%$ at 100 μM and $61.4\% \pm 8.4\%$ at 200 μM compared to untreated controls. For *C. albicans*, metabolic activity decreased to $78.5\% \pm 4.3\%$ at 100 μM and $55.4\% \pm 6.4\%$ at 200 μM . When comparing both species, the lowest metabolic activity for *C. albicans* was observed after 6 hours ($65.4\% \pm 6.0\%$ at 100 μM ; $39.3\% \pm 2.8\%$ at 200 μM), while *C. auris* showed a sustained inhibition across all time points. These results were consistent with fluorescence microscopy findings: HSL treatment markedly suppressed the proliferation of both *C. auris* and *C. albicans* cells relative to untreated controls. In *C. auris* cultures, large aggregates (30–50 cells) appeared after 8 hours of exposure. Interestingly, while HSL did not completely inhibit the dimorphic transition of *C. albicans* (formation of germ tubes, hyphae, and pseudohyphae), it disrupted their structural organization, resulting in irregular and entangled hyphal aggregates after prolonged exposure.

Effect of HSL on *Candida* virulence *in vivo*

To assess the influence of HSL on fungal virulence *in vivo*, a systemic mouse infection model using immunosuppressed BALB/c females was employed. Fungal burdens were determined in kidney homogenates. For *C. albicans*, no statistically significant difference was observed in kidney fungal load between HSL-treated and control groups. In contrast, *C. auris*-infected mice exhibited a marked reduction in viable fungal cell counts following 50 μM and 100 μM HSL treatments compared with untreated controls. Histopathological findings supported these

results. In the kidneys of *C. auris*-infected control animals, extensive tissue damage and budding yeast cells were detected. Daily administration of 50 μ M HSL significantly reduced both the number and severity of these lesions. In *C. albicans*-infected animals, however, multiple and extensive fungal lesions were observed across all treatment groups, containing yeast cells, pseudohyphae, and true hyphae.

Transcriptomic changes in *Candida* species following HSL treatment

To elucidate the molecular mechanisms underlying HSL-induced physiological changes, global transcriptomic analyses were performed for both *C. albicans* and *C. auris*.

For *C. albicans*, 100 μ M HSL treatment resulted in 189 upregulated and 132 downregulated genes, while 200 μ M HSL led to 354 upregulated and 540 downregulated genes. Only limited overlap was observed between the two treatment groups: 44 genes were consistently upregulated and 76 consistently downregulated. At 100 μ M HSL, downregulated genes were primarily associated with the mitotic cell cycle (21 genes), sterol biosynthesis (8 genes; e.g., *ERG1*, *ERG3*), and morphological regulation (*CCNI*, *GIN4*, *HSL1*). Conversely, genes involved in fatty acid degradation (8), RNA metabolism (99), and ribosome biogenesis (73) were upregulated. At 200 μ M, broader transcriptional repression was observed across genes involved in vegetative growth, including mitotic cycle (54 genes), DNA replication (32), RNA metabolism (139), ribosome biogenesis (136), translation (125), sterol biosynthesis (32; e.g., *HMG1*, *ID11*, *CYB5*, *ERG1*, *ERG3*, *ERG6*, *ERG9*, *ERG11*, *ERG12*, *ERG13*), and fatty acid biosynthesis (*FEN12*, *FEN1*, *FAD3*, *EHT1*, *SUR2*, *ERG251*, *LAB5*). Upregulated genes were enriched in pathways related to drug transport (33 genes; *CDR1*, *CDR2*, *SNQ2*, *MRR1*), oxidative stress response (17 genes; *CIP1*, *SOD1*, *SOD2*, *SOD6*, *PST1*), glutathione metabolism (16 genes; *TTR1*, *GST2*, *GPXI*), and fatty acid degradation (13 genes).

For *C. auris*, fewer transcriptional changes were observed. At 100 μ M HSL, 67 genes were upregulated and 111 downregulated, while at 200 μ M, 45 genes were upregulated and 25 downregulated. Only one gene showed consistent upregulation in both species. RT-qPCR validation confirmed high correlation with RNA-seq results (Pearson's $r = 0.92$ – 0.95). In *C. auris*, 200 μ M HSL induced global transcriptomic alterations. Upregulated genes were associated with transmembrane transport (34 genes; including antifungal transporters *CDR1*, *CDR4*, and phosphate transporter *PHO84*), peroxisomal and mitochondrial processes (21 and 40 genes, respectively), iron homeostasis (*FTH1*, *FRE9*, *HMX1*, heme-binding proteins, *RL11*, *ALK2*, cytochrome P450, *CDG1*), and fatty acid β -oxidation (22 genes).

Downregulated genes were primarily involved in transmembrane transport (36), including drug (*MLT1*, *B9J08_003832*), copper and zinc transport (*CTR1*, *ZRT2*, *B9J08_003341*), iron homeostasis (*FRP1*, *FTR1*, *FTP1*, *PGA7*, *B9J08_003002*), glutathione metabolism (*GCSI*, *GLR1*, *APE2*, *RNR3*), DNA replication (9), and antifungal resistance (*MRR1*, *FAS1*, *FAS2*).

Notably, the *B9J08_001458* (*SCF1*) gene—encoding a *C. auris*-specific surface colonization factor—was downregulated under both treatment conditions, while genes related to β -oxidation via 3-hydroxypropionate (*POX1-3*, *FOX2*, *CAT2*, *CRC1*, *HPD1*) were upregulated. At 100 μ M HSL, zinc-binding genes (*SFU1*, *CRZ2*, *ZCF4*, *SUT1*, *IRF1*) were also highly expressed, while genes associated with the pre-replicative complex (*MCM6*, *CDC6*), translation (25), ribosome biogenesis (20), sterol biosynthesis (*ERG2*, *ERG5*, *ERG13*), and drug transport (*MDR1*, *ROA1*) were downregulated.

Changes in intracellular metal concentration following HSL treatment

HSL exposure caused major transcriptional shifts in genes regulating metal ion homeostasis, which were validated by ICP-OES measurements. After 4 hours of exposure, both 100 μ M and 200 μ M HSL significantly reduced intracellular iron and zinc levels in *C. auris* ($p < 0.05$ – 0.001). Iron concentration decreased from 231.6 ± 6.7 μ g/g (control) to 155.0 ± 30.6 μ g/g (100 μ M) and 117.5 ± 12.5 μ g/g (200 μ M). Zinc levels declined from 612.1 ± 19.3 μ g/g (control) to 436.6 ± 54.4 μ g/g (100 μ M) and 326.4 ± 27.8 μ g/g (200 μ M). No significant changes were detected in copper or manganese content. Copper concentrations were 9.7 ± 0.5 μ g/g (control), 11.7 ± 1.8 μ g/g (100 μ M), and 11.6 ± 2.3 μ g/g (200 μ M), while manganese levels were 29.4 ± 0.9 μ g/g (control) and 30.1 ± 1.2 μ g/g (treated; $p > 0.05$). These results indicate that HSL interferes with intracellular iron and zinc homeostasis, which may contribute to its inhibitory effects on *C. auris*.

Discussion

Our research focused on the complex interactions between fungi and bacteria, with particular attention to the processes through which bacteria can inhibit the virulence and other physiological characteristics of *Candida* species. The dynamic relationship between bacteria and fungi can be influenced by direct cell-to-cell contact, the secretion of secondary metabolites, and quorum-sensing molecules. The production and detection of these signaling compounds allow microbial populations to modify their collective behavior in response to changes in their biological or abiotic environment.

Interactions between *Candida* and bacteria are typically antagonistic, often characterized by antifungal, virulence-inhibiting, or even fungicidal effects. Among the commensal fungal species in humans, *Candida albicans* is the most well-known. It colonizes several body sites and mucosal surfaces, yet its overgrowth can lead to severe health problems, particularly during gastrointestinal dysbiosis. Overcolonization of the intestinal tract may serve as the source of invasive *Candida* infections. However, probiotic bacterial species or their secondary metabolites — such as biosurfactants — can prevent *C. albicans* overgrowth. The use of such natural compounds, alone or as adjuvants, could help reduce the excessive use of antifungal drugs and, consequently, the selective pressure contributing to resistance development.

One of the most effective biosurfactants identified to date is surfactin, first isolated from *Bacillus subtilis* ATCC 21332, known for its strong antimicrobial, antitumor, and anticoagulant activities. Although studies on the antifungal effects of surfactin remain limited, existing data suggest that it reduces the cell surface hydrophobicity, adhesion, and biofilm-forming capacity of *C. albicans*. Nevertheless, the detailed physiological and transcriptional mechanisms underlying the antifungal activity of surfactin have remained largely unexplored.

Our results demonstrate that surfactin, produced by *B. subtilis*, plays a significant role in modulating the metabolism and morphogenesis of *C. albicans* and can influence the expression of genes involved in antifungal drug resistance. The observed strong growth inhibition correlated with a general downregulation of genes associated with metabolism. Surfactin treatment markedly affected the transcription of genes related to ribosome biogenesis, which is closely linked to cell growth and division. Gene ontology analysis revealed that surfactin significantly increased the transcription of genes associated with RNA metabolism (220 genes in total), including those related to pre-ribosomal processing, while downregulating genes involved in rRNA transport (10 genes), cytoplasmic ribosomal proteins (69 genes), and translation (128 genes). These transcriptomic findings suggest that the reduced growth rate of

C. albicans cells following surfactin exposure may be related not only to changes in metabolic gene expression but also to the inhibition of protein synthesis.

Several genes associated with ergosterol biosynthesis (*ERG1*, *ERG3*, *ERG9*, *ERG10*, *ERG11*) and fatty acid metabolism (*ACC1*, *FAS1*, *FAS2*) were also downregulated, indicating possible alterations in membrane structure and fluidity. Regarding biofilm formation, the transcription of *EFG1* and *ECE1* was significantly reduced, which may explain the inhibition of hyphal development and biofilm formation observed microscopically.

Our transcriptomic data also revealed that surfactin significantly affected the transcription of genes involved in iron, copper, and zinc transport, as well as the intracellular concentrations of these metals in *C. albicans*. The reduced iron content likely represents part of a general cellular defense strategy against surfactin, aimed at minimizing damage caused by Fe(II)-mediated oxidative stress, for instance by limiting the generation of reactive oxygen species. The decrease in intracellular zinc concentration correlated with the downregulation of *ZRT2*, which encodes the primary zinc transporter in *C. albicans*. Zinc plays a crucial role in oxidative stress protection, as it is a structural component of superoxide dismutase (SOD). Moreover, deletion or repression of *ZRT2* is known to reduce *C. albicans* virulence by diminishing its colonization ability, which may explain the significant reduction in viable fungal cells recovered from mouse kidneys.

Copper homeostasis also represents a key determinant of *C. albicans* virulence. In our study, the transcription of *CTR1* and *FRE7* increased, enhancing the synthesis of copper uptake proteins such as the Ctr1 transporter and Fre7 ferric reductase. Conversely, *CRP1* expression — encoding a P-type ATPase involved in copper efflux — was reduced, suggesting altered copper balance in response to surfactin exposure.

In addition to the Gram-positive *Bacillus*–*Candida* interaction, Gram-negative bacteria also exhibit notable antifungal properties. The relationship between *Pseudomonas aeruginosa* and *C. albicans* has long served as a model for studying fungus–Gram-negative bacterial interactions, typically described as competitive or antagonistic under *in vitro* conditions. Numerous studies have shown that *P. aeruginosa* secretes molecules capable of inhibiting the yeast-to-hypha transition of *C. albicans*. Among these, quorum-sensing molecules such as homoserine lactones mediate microbial communication and are largely responsible for the observed interaction patterns. However, observations from *C. albicans*-based studies cannot be directly extrapolated to mixed populations involving *Pseudomonas* and non-*albicans Candida* species.

A striking example of this difference is *Candida auris*, which efficiently colonizes skin and mucosal surfaces and often coexists with commensal Gram-negative bacteria — including *P. aeruginosa* — without evident antagonism. Nevertheless, data on the clinical and physiological relevance of this bacterial–fungal relationship remain scarce. Our study therefore investigated how *C. auris* responds to *P. aeruginosa*'s primary quorum-sensing molecule, HSL (N-(3-oxododecanoyl)-L-homoserine lactone).

Our results clearly demonstrate that most HSL-induced responses were species-specific for *C. auris*, with only a limited overlap observed with *C. albicans*. Transcriptomic analyses revealed that HSL — regardless of concentration — strongly influenced the expression of genes involved in multidrug transport. In *C. albicans*, 200 μ M HSL induced strong upregulation of *CDR1* and *CDR2*, with significantly higher transcription levels than those observed at 100 μ M. In *C. auris*, both *CDR1* and *CDR4* expression increased markedly under 200 μ M HSL exposure. *CDR1* encodes an ABC efflux pump that plays a key role in azole resistance in *C. albicans*. Interestingly, in *C. auris*, the 100 μ M HSL treatment significantly reduced the transcription of *ROA1*, *MDR1*, and *MRR1*—the latter being a major regulator of azole resistance. These results support the hypothesis that HSL may serve as a potential substrate for these efflux transporters, enabling fungal cells to partially protect themselves against its toxic effects.

With respect to ergosterol content, HSL exerted a stronger inhibitory effect on ergosterol biosynthesis in *C. albicans* than in *C. auris*. In *C. albicans*, HSL — particularly at 200 μ M — led to significant downregulation of *ERG3*, *ERG6*, and *ERG11*, potentially altering sensitivity to antifungal agents targeting the cell membrane.

Adhesion-based experiments revealed that HSL significantly affected both the morphology and metabolic activity of adherent fungal cells. The transcription of the surface colonization factor gene (*SCF1*) decreased following HSL treatment. Since *SCF1* plays a crucial role in the adhesion of *C. auris* to abiotic surfaces, skin, and biofilms, its downregulation likely explains the reduced adhesion and biofilm formation observed in treated cells. Although no major inhibition of hyphal formation was observed in *C. albicans* during the experimental period, treated cells displayed clear morphological alterations compared to untreated controls.

Distinct differences in the transcriptional profiles of metabolism-related genes were also observed between *C. albicans* and *C. auris* following HSL exposure — particularly in fatty acid oxidation pathways. In *C. auris*, over 60% of genes related to fatty acid oxidation were upregulated after HSL treatment, with significant differences between 100 and 200 μ M. These included *FAA21*, *POT1*, and *POXI-3*. By contrast, only about 20% of fatty acid oxidation genes were upregulated in *C. albicans*, and only at 100 μ M HSL. We hypothesize that enhanced fatty

acid utilization and partial degradation of membrane lipids increase metabolic flux, helping to maintain membrane fluidity — especially under conditions of ergosterol gene repression. Our transcriptomic data further suggest that HSL affects the β -oxidation pathway in *C. auris* through mechanisms involving 3-hydroxypropionate metabolism.

To further evaluate the effect of HSL on fungal virulence, we employed an immunosuppressed mouse model. Interestingly, HSL treatment did not influence *C. albicans* virulence *in vivo*, as confirmed by fungal burden measurements and histopathological analysis of the kidneys. In contrast, *C. auris* exhibited a remarkable sensitivity pattern: lower HSL concentrations (50–100 μ M) significantly reduced the number of viable fungal cells in kidney tissue, and the extent of fungal lesions was smaller and less severe compared with untreated controls or the high-concentration (200 μ M) group.

Among all pathways analyzed, fatty acid oxidation was the only one showing significant transcriptional differences between species and treatment concentrations. Fatty acid oxidation is known to be closely associated with *Candida* virulence, as it plays a fundamental role in metabolic adaptation, energy production, immune evasion, and morphogenesis.

Beyond the metabolic differences observed, HSL treatment significantly reduced intracellular iron and zinc levels in *C. auris*, which may contribute to the β -oxidation-related attenuation of virulence at 50–100 μ M. Iron and zinc are critical for the virulence of many human pathogenic fungi, including *Candida* species. These results strengthen the hypothesis that quorum-sensing molecules with 12-carbon backbones, such as HSL, exert broad effects on key fungal physiological processes — including fatty acid oxidation, virulence, and intracellular metal homeostasis — particularly in *C. auris*.

In summary, our findings shed new light on the role of quorum-sensing molecules and secondary metabolites, such as HSL and surfactin, in regulating the pathogenicity and adaptive responses of *Candida* species. The mechanisms identified suggest that these compounds act not only as communication signals but also as fine-tuning regulators within microbial ecosystems. Notably, the ion imbalance and metabolic remodeling observed in *C. auris*, including alterations in fatty acid oxidation, point to previously unknown adaptive mechanisms in this emerging pathogen.

The ability of these molecules to modulate fungal virulence, membrane structure, and stress responses opens new avenues for both probiotic and antifungal research. Further studies are needed to clarify how these molecular interactions influence host immune responses and how they could be harnessed therapeutically. In particular, understanding how quorum-sensing

modulation can reduce pathogen virulence without exerting strong selective pressure — such as that leading to antibiotic resistance—represents a promising direction.

Altogether, our results contribute to a deeper understanding of the adaptive biology of *Candida* species and offer new perspectives on exploiting microbe–microbe and microbe–signal communication as a potential therapeutic strategy.

Summary

In recent years, the study of bacterial–fungal interactions have gained increasing importance, as these relationships play a fundamental role in shaping microbial ecosystems and influencing the outcomes of infections. In our experiments, we investigated the effects of *Pseudomonas aeruginosa*–derived N-(3-oxododecanoyl)-L-homoserine lactone (HSL) and *Bacillus subtilis*–derived surfactin, focusing on how these bacterial molecules may influence the behaviour, virulence, and metabolism of *Candida* species (*Candida albicans* and *C. auris*).

During the investigation of HSL, we found that this quorum-sensing molecule markedly altered the growth, adhesion, and gene expression profiles of *C. auris* and *C. albicans*. HSL treatment led to a reduction in adhesion capacity and biofilm formation, accompanied by the downregulation of several key genes, including *SCF1*. In *C. auris*, large cellular aggregates were observed, whereas in *C. albicans*, distorted hyphal structures appeared. Transcriptomic analyses revealed that HSL primarily affected genes related to fatty acid oxidation, membrane organization, and ion transport, shifting cellular metabolism toward the β -oxidation pathway. The expression of ergosterol biosynthesis genes decreased, potentially leading to changes in membrane fluidity and altered antifungal susceptibility. In parallel, HSL treatment caused a significant reduction in the intracellular iron and zinc content of fungal cells, while several multidrug efflux pump genes (e.g., *CDR1*, *CDR4*) were upregulated. In animal infection models, low concentrations of HSL (50–100 μ M) reduced the fungal burden of *C. auris* in mouse kidneys, while no similar effect was observed for *C. albicans*.

Surfactin, the cyclic lipopeptide produced by *B. subtilis*, also demonstrated strong antifungal activity. Even after short exposure, surfactin inhibited the growth, adhesion, hyphal development, and biofilm formation of *C. albicans*. Intracellular iron, manganese, and zinc levels decreased, while glutathione levels increased. Transcriptomic profiling revealed downregulation of genes associated with ergosterol and fatty acid biosynthesis (*ERG1*, *ERG3*, *FAS1*), as well as biofilm formation (*EFG1*, *ECE1*). Moreover, surfactin acted synergistically with fluconazole, further enhancing antifungal efficacy.

Collectively, both studies emphasize that bacterial signal molecules function not merely as communication mediators but as complex cellular regulators that profoundly influence fungal metabolism and pathogenicity. These findings highlight that the targeted modulation of such interactions could offer novel strategies for controlling *Candida* infections and mitigating antifungal resistance.

New Findings

- Surfactin, produced by *Bacillus subtilis*, markedly inhibited the virulence of *Candida albicans* by reducing adhesion, morphogenesis, and biofilm formation.
- Transcriptomic profiling revealed that surfactin treatment downregulated genes involved in ergosterol and fatty acid biosynthesis, as well as genes associated with biofilm development.
- The quorum-sensing molecule HSL, produced by *Pseudomonas aeruginosa*, significantly affected the growth, adhesion, and gene expression of *C. auris* and *C. albicans*, thereby substantially reducing fungal virulence.
- Transcriptomic analyses indicated that HSL primarily modulates the transcription of genes related to membrane integrity, ion transport, and fatty acid oxidation, shifting the overall metabolic activity toward the β -oxidation pathway.
- Under *in vivo* conditions, low concentrations of HSL effectively inhibited *C. auris* invasion and tissue-damaging capacity.

Acknowledgments

Learning and research often demand significant sacrifices—not only from the person directly involved, but also from everyone who, whether directly or indirectly, becomes part of this long and demanding journey. Many people quietly stand behind you, offering support and walking alongside you the entire way. I believe this is true in many areas of life, and it was certainly true throughout the preparation of this dissertation. For that reason, this doctoral work reflects not only my own efforts, but also the invaluable help of all those who guided and supported me.

First and foremost, I am deeply grateful to my supervisor, Renátó Kovács, for standing by me both professionally and personally over the past four years. He introduced me to this research topic, and his advice and encouragement greatly contributed to my scientific progress and development.

I would also like to express my sincere thanks to my boss, József Kónya, who made it possible for me to conduct my doctoral research at the Institute of Medical Microbiology alongside my diagnostic work. I am grateful to László Majoros, Head of the Mycology Laboratory, for welcoming me into the “fungal lab,” and for supporting my work with his professional insight. My heartfelt thanks go to all colleagues in the Mycology Laboratory for the many forms of expert help and support I received over the years. I am especially indebted to Ágnes Jakab, whose guidance and support contributed greatly to the success of my research. I thank Fruzsina Nagy and Zoltán Tóth for introducing me to the *in vitro* research conducted in the Mycology Laboratory and for their advice over the years. I also wish to thank Lajos Forgács and Dávid Balázs for their assistance and support in the *in vivo* experiments. I am personally grateful to Noémi Balla and Andrea Harmath for their collaboration and for the help they provided throughout my research work.

Special thanks are due to Ágota Ragyák and Zsófia Sajtos of the Department of Inorganic and Analytical Chemistry, Institute of Chemistry, Faculty of Science and Technology, University of Debrecen, as well as to the staff of the Genomic Medicine and Bioinformatics Service Laboratory, Faculty of Medicine, University of Debrecen, for their assistance with various aspects of this research.

I would also like to thank Andrew M. Borman for generously providing the *Candida auris* isolates included in our strain collection, and Ákos T. Kovács for his professional support with our *Bacillus subtilis* experiments.

My thanks extend to all former and current colleagues at the Institute of Medical Microbiology who supported my PhD work and encouraged me throughout these four years.

Finally, and most importantly, I am profoundly grateful to my family and friends, who stood by me unwaveringly, offering support, encouragement, patience, and understanding even in the most difficult times. Without their love and support, this dissertation would not have been possible.

This work was supported by the National Research, Development and Innovation Office (NKFIH FK138462, TKP2021-EGA) and by the New National Excellence Program (UNKP-21-5-DE-473) financed by the National Research, Development and Innovation Fund. We also acknowledge funding from the Complex Health Industry Multidisciplinary Competence Centre (GINOP-2.3.4-15-2020-00008).



Registry number: DEENK/573/2025.PL
Subject: PhD Publication List

Candidate: Fruzsina Kovács
Doctoral School: Doctoral School of Pharmacy
MTMT ID: 10082691

List of publications related to the dissertation

1. **Kovács, F.**, Jakab, Á., Balla, N., Tóth, Z., Balázsi, D., Forgács, L., Harmath, A., Bozó, A., Ragyák, Á., Majoros, L., Kovács, R. L.: A comprehensive analysis of the effect of quorum-sensing molecule 3-oxo-C12-homoserine lactone on *Candida auris* and *Candida albicans*.
Biofilm. 9, 1-12, 2025.
DOI: <http://dx.doi.org/10.1016/j.biofilm.2025.100259>
IF: 4.9 (2024)
2. Jakab, Á., **Kovács, F.**, Balla, N., Tóth, Z., Ragyák, Á., Sajtos, Z., Csillag, K., Nagy-Köteles, C., Nemes, D., Bácskay, I., Pócsi, I., Majoros, L., Kovács, Á. T., Kovács, R. L.: Physiological and transcriptional profiling of surfactin exerted antifungal effect against *Candida albicans*.
Biomed. Pharmacother. 152, 1-10, 2022.
DOI: <http://dx.doi.org/10.1016/j.biopha.2022.113220>
IF: 7.5

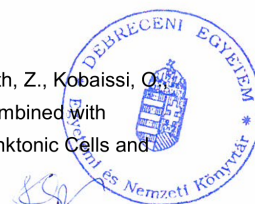
List of other publications

3. Balla, N., **Kovács, F.**, Tóth, Z., Harmath, A., Bozó, A., Majoros, L., Kovács, R. L., Jakab, Á.: Isolate Specific Transcriptome Changes Exerted by Isavuconazole Treatment in *Candida auris*.
Mycopathologia. 190 (1), 1-11, 2025.
DOI: <http://dx.doi.org/10.1007/s11046-024-00919-1>
IF: 2.9 (2024)
4. Jakab, Á., **Kovács, F.**, Balla, N., Nagy-Köteles, C., Ragyák, Á., Nagy, F., Borman, A. M., Majoros, L., Kovács, R. L.: Comparative transcriptional analysis of *Candida auris* biofilms following farnesol and tyrosol treatment.
Microbiol. Spectr. 12 (4), 1-12, 2024.
DOI: <https://doi.org/10.1128/spectrum.02278-23>
IF: 3.8





5. **Kovács, F.**, Balla, N., Bozó, A., Harmath, A., Jakab, Á., Tóth, Z., Nagy, F., Majoros, L., Kovács, R. L.: Epidemiology, clinical characteristics, outcome and biofilm forming properties in candidaemia: a single-centre retrospective 4-year analysis from Hungary. *Mycoses*. 67 (4), 1-12, 2024.
DOI: <http://dx.doi.org/10.1111/myc.13727>
IF: 3.1
6. Balázs, D., Tóth, Z., Locke, J. B., Borman, A. M., Forgács, L., Balla, N., **Kovács, F.**, Kovács, R. L., Amano, C., Baran, T. I., Majoros, L.: In Vivo Efficacy of Rezafungin, Anidulafungin, Caspofungin, and Micafungin against Four *Candida auris* Clades in a Neutropenic Mouse Bloodstream Infection Model. *J. Fungi*. 10 (9), 1-14, 2024.
DOI: <http://dx.doi.org/10.3390/jof10090617>
IF: 4
7. Demeter, F., Török, P., Kiss, A., Kovásznai-Oláh, R., Máthéné Szigeti, Z., Baksa, V., **Kovács, F.**, Balla, N., Fenyvesi, F., Váradi, J., Borbás, A., Herczeg, M.: First Synthesis of DBU-Conjugated Cationic Carbohydrate Derivatives and Investigation of Their Antibacterial and Antifungal Activity. *Int. J. Mol. Sci.* 24 (4), 1-20, 2023.
DOI: <http://dx.doi.org/10.3390/ijms24043550>
IF: 4.9
8. Balla, N., Jakab, Á., **Kovács, F.**, Ragyák, Á., Tóth, Z., Balázs, D., Forgács, L., Bozó, A., Al Refai, F., Borman, A. M., Majoros, L., Kovács, R. L.: Total transcriptome analysis of *Candida auris* planktonic cells exposed to tyrosol. *AMB Express*. 13 (1), 1-10, 2023.
DOI: <http://dx.doi.org/10.1186/s13568-023-01586-z>
IF: 3.5
9. Kovács, R. L., Erdélyi, L. J., Fenyvesi, F., Balla, N., **Kovács, F.**, Vámosi, G., Klusóczki, Á., Gyöngyösi, A., Bácskay, I., Vecseryés, M., Váradi, J.: Concentration-Dependent Antibacterial Activity of Chitosan on *Lactobacillus plantarum*. *Pharmaceutics*. 15 (1), 1-11, 2022.
DOI: <http://dx.doi.org/10.3390/pharmaceutics15010018>
IF: 5.4
10. Balla, N., **Kovács, F.**, Balázs, B., Borman, A. M., Bozó, A., Jakab, Á., Tóth, Z., Kobaissi, O., Majoros, L., Kovács, R. L.: Synergistic Interaction of Caspofungin Combined with Posaconazole against FKS Wild-Type and Mutant *Candida auris* Planktonic Cells and Biofilms. *Antibiotics-Basel*. 11 (11), 1-12, 2022.
DOI: <http://dx.doi.org/10.3390/antibiotics11111601>
IF: 4.8





11. Jakab, Á., Balla, N., Ragyák, Á., Nagy, F., **Kovács, F.**, Sajtos, Z., Tóth, Z., Borman, A. M., Pócsi, I., Baranyai, E., Majoros, L., Kovács, R. L.: Transcriptional profiling of the *Candida auris* response to exogenous farnesol exposure.
mSphere. 6 (5), 1-12, 2021.
DOI: <http://dx.doi.org/10.1128/mSphere.00710-21>
IF: 5.029

Total IF of journals (all publications): 49,829

Total IF of journals (publications related to the dissertation): 12,4

The Candidate's publication data submitted to the Tudóstér have been validated by DEENK on the basis of the Journal Citation Report (Impact Factor) database.

06 November, 2025

